



This is a repository copy of *Towards the prediction of spontaneous preterm birth by cervical collagen imaging using polarization-sensitive OCT.*

White Rose Research Online URL for this paper:

<https://eprints.whiterose.ac.uk/226805/>

Version: Accepted Version

---

### Proceedings Paper:

Hooper, F.S., Revin, D.G., Theofrastou, E. et al. (5 more authors) (2025) Towards the prediction of spontaneous preterm birth by cervical collagen imaging using polarization-sensitive OCT. In: Ramella-Roman, J.C., Ma, H., Vitkin, I.A., Elson, D.S. and Novikova, T., (eds.) Polarized Light and Optical Angular Momentum for Biomedical Diagnostics 2025. BIOS, 2025, 25-31 Jan 2025, San Francisco, California, United States. Proceedings of SPIE, 13322 . SPIE , p. 1332206. ISBN 9781510683921

<https://doi.org/10.1117/12.3041117>

---

© 2025 The Authors. Except as otherwise noted, this author-accepted version of a paper published in Proceedings of SPIE: Polarized Light and Optical Angular Momentum for Biomedical Diagnostics 2025 is made available via the University of Sheffield Research Publications and Copyright Policy under the terms of the Creative Commons Attribution 4.0 International License (CC-BY 4.0), which permits unrestricted use, distribution and reproduction in any medium, provided the original work is properly cited. To view a copy of this licence, visit <http://creativecommons.org/licenses/by/4.0/>

### Reuse

This article is distributed under the terms of the Creative Commons Attribution (CC BY) licence. This licence allows you to distribute, remix, tweak, and build upon the work, even commercially, as long as you credit the authors for the original work. More information and the full terms of the licence here:

<https://creativecommons.org/licenses/>

### Takedown

If you consider content in White Rose Research Online to be in breach of UK law, please notify us by emailing [eprints@whiterose.ac.uk](mailto:eprints@whiterose.ac.uk) including the URL of the record and the reason for the withdrawal request.



[eprints@whiterose.ac.uk](mailto:eprints@whiterose.ac.uk)  
<https://eprints.whiterose.ac.uk/>

# Towards the prediction of spontaneous preterm birth by cervical collagen imaging using polarization sensitive OCT

Frances S.W. Hooper <sup>\*a</sup>, Dmitry G. Revin <sup>a</sup>, Efstratios Theofrastou <sup>b</sup>, Niraj K. Soni <sup>a</sup>, Rui Yuan <sup>a</sup>,  
Vanessa Hearnden <sup>c</sup>, Dilly O.C. Anumba <sup>b</sup>, Stephen J. Matcher <sup>a</sup>

<sup>a</sup> School of Electrical and Department of Electronic and Electrical Engineering, Sir Frederick Mappin Building, University of Sheffield, Sheffield, S1 3JD4DT, UK; <sup>b</sup> Academic Unit of Reproductive and Developmental Medicine, University of Sheffield, Sheffield, S10 2SF, UK; <sup>c</sup> School of Chemical, Materials and Biological Engineering, Kroto Research Institute, University of Sheffield, Sheffield, S3 7HQ, UK

## ABSTRACT

**Introduction:** Preterm birth (PTB) remains one of the leading risk factors of neonatal mortality despite the ongoing research to reduce its incidence. Spontaneous PTB (sPTB) can arise as a result of premature remodeling of the collagen-rich extracellular matrix (ECM) of the cervix. Non-invasive biomarkers of cervical collagen content, such as birefringence, may thus have diagnostic value in predicting sPTB. In our previous work, we showed that polarization-sensitive OCT (PS-OCT) can characterize *in vitro* cervical collagen alignment through measurements of the backscattered light's polarization state, differentiating collagen from the surrounding ECM of the cervical epithelium. To advance this towards *in vivo* measurements, we have developed a PS-OCT system, based on Jones Matrix calculus (JM-OCT), which is an extension of PS-OCT optimized for fiber-optic beam delivery. We have coupled this to an in-house designed colposcopic probe, to characterize changes in cervical collagen organization during term and preterm pregnancies. This study aims to assess the performance of this system prior to clinical studies.

**Methods:** JM-OCT images of several material and biological samples with expected birefringent properties and depth-based landmarks were obtained with the colposcopic probe, including *in vitro* ovine cervix. OCT B-scans containing 700 A-scans were acquired with filtered phase retardance to assess the system's resolution, imaging depth and area, and ability to present changes in sample birefringence.

**Results:** The system successfully produced high intensity OCT B-scans with high axial resolution (14  $\mu\text{m}$ ) and imaging depth (up to 2.1 mm), displaying depth-resolved landmarks including blood vessels within the *in vivo* skin's papillary dermis. Changes in material and ECM birefringence were clearly displayed in phase retardance images.

**Conclusion:** The performance of our in-house designed colposcopic probe coupled with the in-house built JM-OCT engine shows great potential to image *in vivo* cervical collagen orientation and abundance in future studies. With its high axial resolution and phase retardance imaging, we aim to investigate the application of our imaging system clinically, to assess its value in understanding, predicting, and preventing PTB.

**Keywords:** polarization sensitive optical coherence tomography, colposcopic probe, Jones matrix calculus, preterm birth, cervical collagen,

## 1. INTRODUCTION

Preterm birth (PTB), the delivery of a neonate prior to 37 weeks gestation, remains one of the leading global risk factors of morbidity and mortality in children under 5 years old. In 2022, 13.4 million global live births were premature <sup>1</sup>, and in England and Wales, neonatal mortality rates were 2.9 in every 1000 live birth, with 29.5% of all neonatal deaths occurring in infants born prior to 24 weeks gestation <sup>2</sup>. PTB can be characterized by its spontaneity, with iatrogenic PTB being intentionally and medically initiated due to maternal illness or fetal distress <sup>3</sup>, and spontaneous PTB (sPTB), which is reported to result in 47-70% of overall PTBs <sup>3,4</sup>. Although sPTB can be caused by the preterm premature rupturing of membranes (PPROM), 40-45% of PTBs were caused by spontaneous preterm labor, either following PPRM or with

intact membranes<sup>4</sup>. Despite the multitude of factors associated with preterm labor, ranging from maternal demographics and medical history to infection and inflammation, screening for one singular cause or risk factor cannot guarantee the prediction and prevention of sPTB<sup>5</sup>. Instead, we aim to build on the understanding that the cervix must undergo a physiologically activated change that can start weeks to months before active at term<sup>6</sup>. This change, named cervical remodeling, describes the progression of the firmly closed cervix, through cervical softening and ripening, to dilation and labor, by the reduction of collagen concentration and cross-linking within the cervixes extracellular matrix (ECM)<sup>7, 8</sup>. Assessing non-invasive biomarkers of cervical collagen content, such as birefringence, during this remodeling, may thus have diagnostic value in predicting sPTB.

To achieve this, polarization imaging techniques can be implemented. Previous studies using linearly polarized light colposcopy have successfully characterized circumferential collagen alignment in the middle zone of the non-pregnant cervix<sup>9</sup>. Additionally, Mueller matrix imaging has successfully tracked cervical ECM remodeling in mice by imaging Mueller polarimetry, despite its limited penetration depth<sup>10</sup>. In previous work, we showed that polarization-sensitive OCT (PS-OCT) can characterize *in vitro* cervical collagen alignment through measurements of the backscattered light's polarization state, differentiating collagen from the surrounding ECM of the cervical epithelium<sup>11</sup>. To further progress with this research, we have developed an OCT compatible colposcopic probe, designed for clinical cervical assessment, introduced in a previous proceeding<sup>12</sup>. To evaluate this probe and advance towards *in vivo* measurements, we have developed a PS-OCT system, based on Jones Matrix calculus (JM-OCT). This system is an extension of PS-OCT, optimized for fiber-optic beam delivery<sup>13</sup>.

## 2. METHODS

### 2.1 Optical colposcopic probe

A handheld colposcopic probe was developed in-house for integration with our polarization-sensitive OCT system for forward-facing sample imaging. The scanning probe's optical layout, shown in Figure 1 was designed using OpticStudio (Ansys, USA). It utilizes a single-mode fiber compatible fixed focus collimator, MEMS scanning mirror, and "focus lens", all anti-reflection coated for 1310 nm wavelength. The probe was designed to allow the scanning beam to be propagated from the external, "handle" region of the probe through the vagina via a narrow 158 mm long endoscopic gradient index (GRIN) lens and projected onto the cervix. OpticStudio optimization and analyses tools were used to assess the *in silico* design and provide the key performance metrics listed in Table 1 for comparison to the realized prototype.

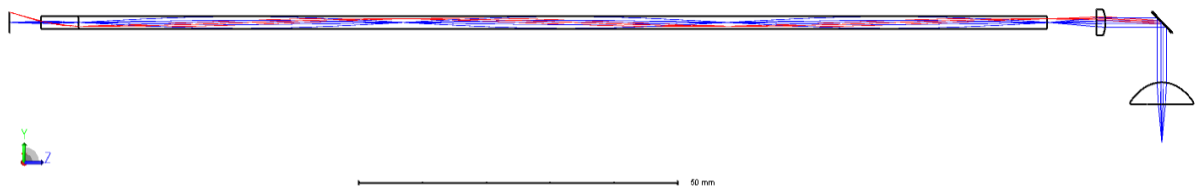


Figure 1. OpticStudio ray trace schematic of colposcopic probe optics.

Table 1. Key performance metrics of simulated probe design, optimized for minimal light loss at fixed working distance with a maximum scanning angle of 2°

Probe design iteration	Lateral resolution/ $\mu\text{m}$		Chief ray incident angle/ $^{\circ}$	Vertical FOV/ $\text{mm}$	Light loss (vignetting) / %	
	on-axis	at + 2°	at + 2°	at + 2°	on-axis	at + 2°
Fixed 5 mm working distance (optimized for on-axis beam)	22.66	32.42	-16.03	3.22	0.00	7.44

The handheld probe casing was designed and built prioritizing patient comfort, clinician usability and clinical hygiene along with optical layout compatibility. This resulted in a slimline prototype providing optical stability for pairing with our in-house OCT systems for performance analysis.

## 2.2 Jones-Matrix OCT imaging

The colposcopic probe was coupled with our in-house built Jones-Matrix OCT (JM-OCT) engine (Figure 2) for fast-axis intensity and phase retardance imaging, similar to <sup>13</sup>. The JM-OCT engine is a fiber-optic based system constructed with a 1310 nm center wavelength MEMS VCSEL laser (Thorlabs, Germany), with a 100 kHz sweep rate, ~100 nm sweeping range and >60% duty cycle. To obtain a sufficient imaging field of view (FOV), the system's scan width was set to 7 mm. The reference arm was constructed with a matching fixed focus collimator to the probe and an adjustable mirror, set 200 mm from the collimator and separated by 127 mm of N-SF1 glass.

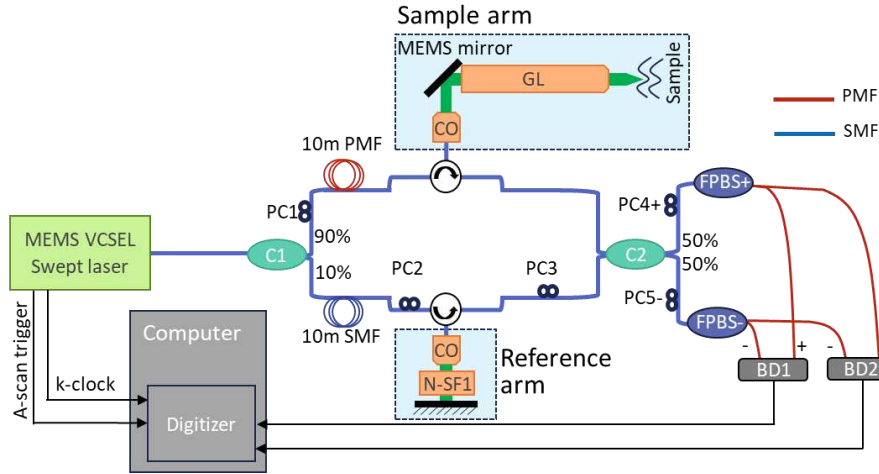


Figure 2. Fiber-based JM-OCT system schematic. Abbreviations: C: coupler, PC: polarization controller, PMF: polarization maintaining fiber, SMF: single mode fiber, CO: collimator, GL: GRIN lens, FPBS: fiber polarization beam splitter, BD balanced detector.

Polarization multiplexing is created by using a polarization maintaining fiber (PMF) in the sample arm. The light beams from the sample and reference arms are recombined at the 50/50 (C2) coupler, and the horizontal and vertical polarizations interference signals are independently detected by the two balanced detectors (BD).

Two raw OCT B-scans containing 700 A-scans were produced by the balanced detectors. Each raw B-scan carries two depth-encoded image copies which were separated by the searching of two images with maximum cross-correlation. The resulting intensity images were acquired by averaging of four separated intensity images and phase retardance images were calculated using Jones calculus [13] and filtered by a 3x5 median filter. The number of phase shift “band” periods per mm imaging depth in the retardance images were then assessed <sup>14</sup>.

## 2.3 Sample Imaging

To fully assess the system, several different biological and non-biological material samples were imaged using the colposcopic probe. To calculate the FOV achieved with the probe, a sample with grated surface relief with a pitch of 0.265 mm was imaged and the number of pitches visible in the intensity images were counted. To determine the lateral resolution of the probe, a USAF 1951 target was imaged through the colposcopic probe coupled with another in-house built OCT system. This high-speed functional OCT angiography (OCTA) system, with a 1310 nm Fourier-Domain Mode Locking (FDML) laser, implements both fast, and slow, scanning axes of the MEMS scanning mirror, allowing for the acquisition of en face imaging of samples.

Other studied non-biological materials included white molded plastic samples that exhibited strong birefringent behaviors. These plastic samples were used to illustrate changes in phase retardance and birefringent uniformity due to inbuilt remaining stress.

The biological samples comprised of *in vivo* skin of the hand and *ex vivo* ovine cervical samples. By imaging the human skin, the system's ability to differentiate between different skin layers and depth resolved landmarks within the dermis could be analyzed. Skin samples included the dorsal hand, palmer hand, and finger pad.

To aid translation into clinic, *ex vivo* ovine cervixes were imaged. The ovine pelvic tract samples were obtained from a local abattoir, from animals being slaughtered for human consumption. The samples were collected on the day of slaughter and transferred to the laboratory in double-sealed plastic containers. Following dissection to remove excess tissue (peritoneal fat and skin), the samples were stored in a sterile phosphate-buffered solution with 0.1 mg/mL streptomycin, 0.25  $\mu\text{g/mL}$  amphotericin B and 100 IU/mL penicillin to prevent bacterial and fungal growth. They were stored for 24 hours at 3  $^{\circ}\text{C}$ , in a fridge designated for animal tissues. The samples were then removed from the solution and OCT data collection was carried out at room temperature. To simulate the clinical application and navigation of the probe, fully intact productive tracks of ewes were used in addition to dissected cervixes.

### 3. RESULTS

#### 3.1 Performance metrics

The axial resolution of the system was found to be 14  $\mu\text{m}$ , with an imaging depth of up to 2.1 mm (in air). Through *en face* imaging of the USFA target with the OCTA system, the lateral resolution of the colposcopic probe was found to be 44.19  $\mu\text{m}$  (Figure 3). Figure 4b shows the intensity image of the grating material sample, counting 12 distinct pitches of 0.265 mm in thickness, giving a system FOV of 3.3 mm for a single B-scan consisting of 700 A-scans. It was previously found that increasing the FOV of the probe reduced its lateral resolution<sup>12</sup>, which may account for the bench tested results having a high FOV and lower lateral resolution than the simulated results from Table 1.

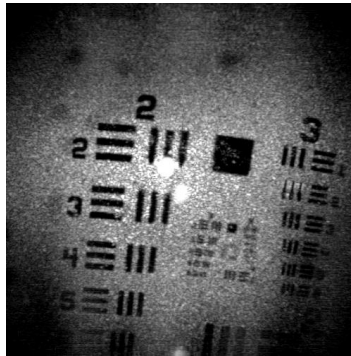


Figure 3. OCTA *en face* imaging of USAF target for lateral resolution assessment of the probe. The lateral resolution of the system is designated as group 4 element 4.

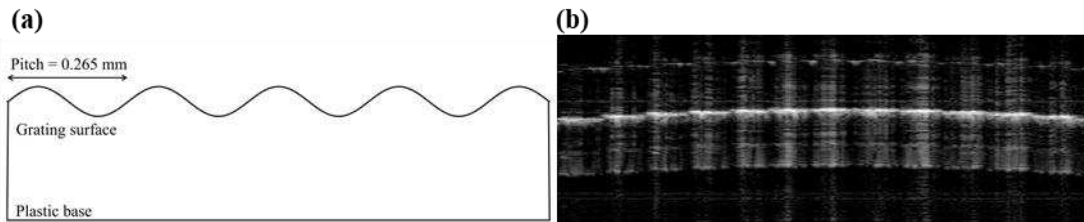


Figure 4. Imaged plastic grating for field of view analysis: (a) diagram of sample from<sup>12</sup> and (b) OCT intensity image.

#### 3.2 Intensity and Phase Retardance imaging

The OCT system was initially assessed using an array of molded plastic samples with strong birefringent behavior (Figure 5). An opaque plastic sample with strong non-uniform changes in birefringence was first studied to assess the system's ability to produce phase retardance images (Figure 5d). The image displays dense, uniform phase retardance banding close to the surface, averaging  $\sim 2.33$  periods of the phase change per mm, indicating high birefringence. Figure 5b and e represent the same sample but at different positions with more localized stress, causing a disruption in the uniformity of the phase retardance band pattern, and random depolarization with increased sample depth. At either side of the affected area high birefringence is suggested by the high phase change frequency near the surface (4.99 - 5.05

periods per mm), although this too decays into random depolarizing with increased depth. In comparison, the translucent tape (Figure 5f) produced a single-phase shift throughout the total imaging depth, indicating much lower birefringence (0.37 phase change periods per mm).

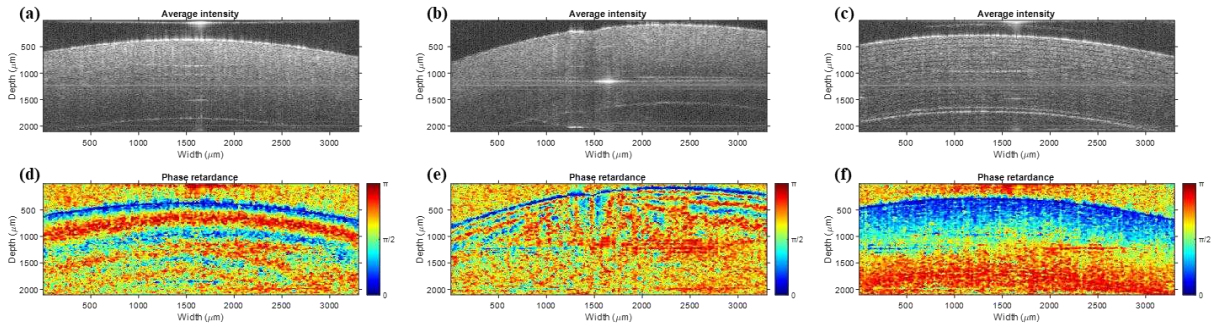


Figure 5. JM-OCT images of plastic samples collected using the colposcopic probe: Opaque plastic bottle cap (a) intensity and (d) phase retardance; Plastic cap with localized stress (b) intensity; and (e) phase retardance; and Translucent scotch tape roll (c) intensity and (f) phase retardance

Figure 6 illustrates the use of the JM-OCT system and probe for intensity and phase retardance imaging of the skin. The dermatological use of OCT is well established, allowing for the assessment of the intensity imaging capabilities of the system<sup>15</sup>. Compared to previous work with other our in-house build OCT systems<sup>16</sup>, distinct layering of the skin is determined, including the epidermis (ED) and dermis (D) in both skin regions and the stratus corneum (SC) in the palm (Figure 6b). Additionally, depth resolved landmarks including blood vessels in the papillary dermis of Figure 6a are visible. The phase retardance results (Figure 6c and d) show that there is a great contrast across different skin regions, and between the dermis and other skin layers. In the dorsal hand skin (Figure 6c), a single phase retardance shift from the epidermis to the dermis is noticeable across most of the A-scans, similar to Figure 5f, although the shift is much faster in this instance. The epidermis of the palmer hand skin (Figure 6d) displays very distinguishable patterns of high phase retardance “ribbons”, that have previously been observed in healthy finger pad PS-OCT images<sup>17</sup>, followed by random depolarization in the dermis.

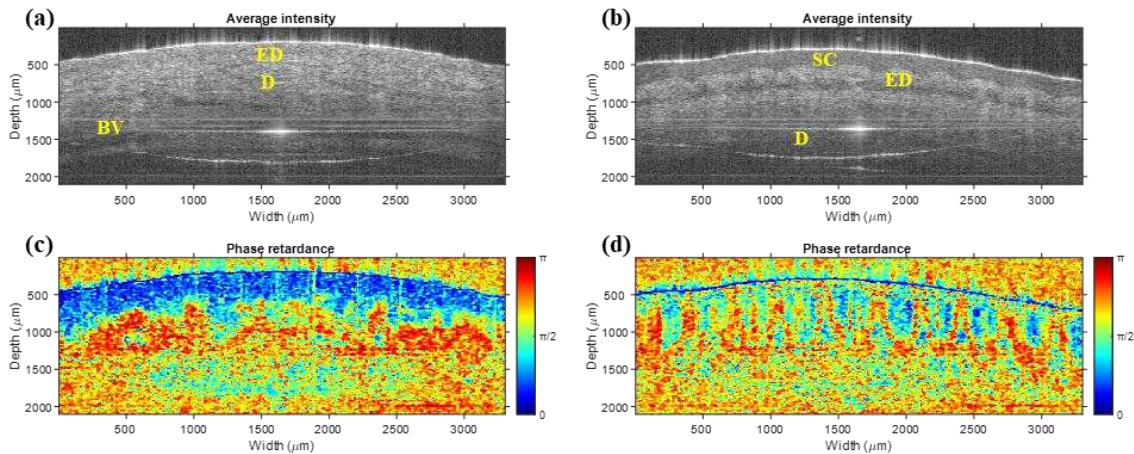


Figure 6. JM-OCT images of *in vivo* skin samples collected using the colposcopic probe: Dorsal hand (a) intensity and (c) phase retardance; and Palmer hand (b) intensity and (d) phase retardance. Abbreviations: stratus corneum (SC), epidermis (ED), dermis (D), and blood vessel (BV).

To establish the viability of the system to image changes in birefringence in cervical tissue, a dissected *in vitro* ovine cervix sample was imaged with the colposcopic probe (Figure 7). The phase retardance image (Figure 7b) displays clear

phase retardance banding indicating strong birefringence near the surface of the sample (1.83 phase change periods per mm), however no birefringent properties are displayed below ~1.5 mm depth. These results build on our previous work that inspired this project, displaying similar phase retardance results obtained from their *in vitro* human studies <sup>11</sup>.

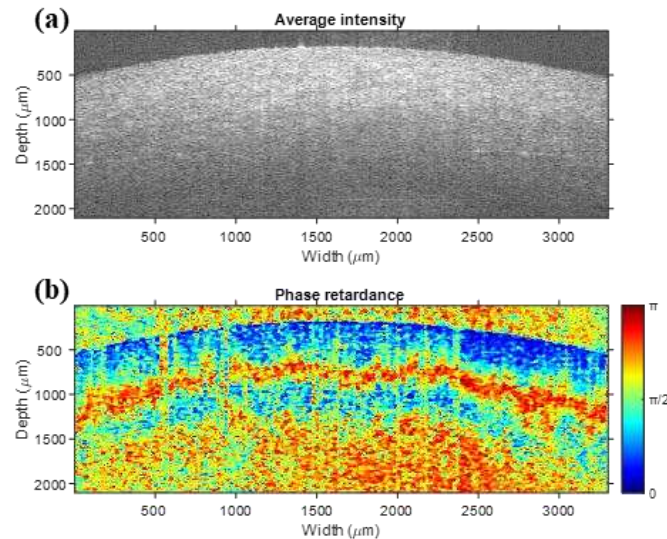


Figure 7. JM-OCT images of dissected *in vitro* ovine cervix collected using the colposcopic probe: (a) intensity and (b) phase retardance.

#### 4. CONCLUSION

We have demonstrated that the performance of our in-house designed and built colposcopic probe provides sufficiently high axial and lateral resolution and FOV for performing OCT imaging of various materials. When coupled with our in-house built JM-OCT engine, the full system was able to produce clear intensity images with depth resolved landmarks in the skin and display the various strengths of changing birefringence in biological and non-biological samples. Most notably, the system performed well on ovine cervical samples, providing collagen imaging evidence. The system shows great potential to image *in vivo* cervical collagen orientation and abundance in future studies, investigating the clinical application of the system and assessing its value in understanding, predicting, and preventing SPTB.

#### ACKNOWLEDGEMENTS

We would like to thank EPSRC (EP/V010581/1) for funding this project, the university of Sheffield for housing us and our systems during their design and development, and the Jessop's Wing for working hard towards getting clinical approval and ethics for us to further our research with the approached aid of clinical patients.

#### REFERENCES

1. E. O. Ohuma et al., "National, regional, and global estimates of preterm birth in 2020, with trends from 2010: a systematic analysis," *The Lancet* **402**(10409), 1261-1271 (2023). [https://doi.org/10.1016/s0140-6736\(23\)00878-4](https://doi.org/10.1016/s0140-6736(23)00878-4).
2. Office for National Statistics (ONS), "Child and infant mortality in England and Wales: 2022," (2024).
3. H. Aughey et al., "Iatrogenic and spontaneous preterm birth in England: A population-based cohort study," *BJOG: An International Journal of Obstetrics & Gynaecology* **130**(1), 33-41 (2023). <https://doi.org/10.1111/1471-0528.17291>.
4. R. L. Goldenberg et al., "Epidemiology and causes of preterm birth," *The Lancet* **371**(9606), 75-84 (2008). [https://doi.org/10.1016/s0140-6736\(08\)60074-4](https://doi.org/10.1016/s0140-6736(08)60074-4).

5. R. Romero, S. K. Dey and S. J. Fisher, "Preterm labor: One syndrome, many causes," *Science* **345**(6198), 760-765 (2014). <https://doi.org/10.1126/science.1251816>.
6. J. Félix, C. Bartosch and A. Matias, "Unlocking the Cervix: Biological Mechanisms and Research Gaps in Preterm Birth," *Cureus* (2024). <https://doi.org/10.7759/cureus.72835>.
7. S. M. Yellon, "Contributions to the dynamics of cervix remodeling prior to term and preterm birth," *Biology of Reproduction* **96**(1), 13-23 (2016). <https://doi.org/10.1095/biolreprod.116.142844>.
8. C. P. Read et al., "Cervical remodeling during pregnancy and parturition: molecular characterization of the softening phase in mice," *Reproduction* **134**(2), 327-340 (2007). <https://doi.org/10.1530/REP-07-0032>.
9. C. P. N. Khuong et al., "Rapid and efficient characterization of cervical collagen orientation using linearly polarized colposcopic images," *Journal of Innovative Optical Health Sciences* **16**(05)(2023). <https://doi.org/10.1142/s1793545822410012>.
10. H. R. Lee et al., "Mueller matrix imaging for collagen scoring in mice model of pregnancy," *Scientific Reports* **11**(1)(2021). <https://doi.org/10.1038/s41598-021-95020-8>.
11. W. Li et al., "Polarization-sensitive optical coherence tomography with a conical beam scan for the investigation of birefringence and collagen alignment in the human cervix," *Biomedical Optics Express* **10**(8), 4190-4206 (2019). <https://doi.org/10.1364/BOE.10.004190>.
12. F. S. Hooper et al., "Optical design and simulation of a cervical scanning probe for polarization-sensitive optical coherence tomography using Ansys Zemax OpticStudio," <https://doi.org/10.1117/12.2670355>.
13. Z. Wang et al., "Depth-encoded all-fiber swept source polarization sensitive OCT," *Biomedical Optics Express* **5**(9), 2931-2949 (2014). <https://doi.org/10.1364/BOE.5.002931>.
14. E. Real et al., "Identification of Human Pathological Mitral Chordae Tendineae Using Polarization-sensitive Optical Coherence Tomography," *Sensors* **19**(3), 543 (2019). <https://doi.org/10.3390/s19030543>.
15. B. Wan et al., "Applications and future directions for optical coherence tomography in dermatology\*," *British Journal of Dermatology* **184**(6), 1014-1022 (2021). <https://doi.org/10.1111/bjd.19553>.
16. D. G. Revin et al., "Visible-light optical coherence tomography platform for the characterization of the skin barrier," *Biomedical Optics Express* **14**(8), 3914-3923 (2023). <https://doi.org/10.1364/BOE.494356>.
17. X. Zhou et al., "Light polarization interaction with skin conditions assessed by polarization sensitive optical coherence tomography," in OSA Technical Digest, *Biophotonics Congress 2021 NTh1C.2* (2021), <https://doi.org/10.1364/NTM.2021.NTh1C.2>.